THE ASTROPHYSICAL JOURNAL, 619:L1–L6, 2005 January 20

THE *GALAXY EVOLUTION EXPLORER*: A SPACE ULTRAVIOLET SURVEY MISSION

D. CHRISTOPHER MARTIN,[1] JAMES FANSON,[2] DAVID SCHIMINOVICH,[1] PATRICK MORRISSEY,[1] PETER G. FRIEDMAN,[1]
TOM A. BARLOW,[1] TIM CONROW,[1] ROBERT GRANGE,[3] PATRICK N. JELINSKY,[4] BRUNO MILLIARD,[3]
OSWALD H. W. SIEGMUND,[4] LUCIANA BIANCHI,[5] YONG-IK BYUN,[6] JOSE DONAS,[3] KARL FORSTER,[1]
TIMOTHY M. HECKMAN,[5] YOUNG-WOOK LEE,[6] BARRY F. MADORE,[7,8] ROGER F. MALINA,[3]
SUSAN G. NEFF,[9] R. MICHAEL RICH,[10] TODD SMALL,[1] FRANK SURBER,[2]
ALEX S. SZALAY,[5] BARRY WELSH,[4] AND TED K. WYDER[1]
Received 2004 June 9; accepted 2004 October 1; published 2005 January 17

ABSTRACT

We give an overview of the *Galaxy Evolution Explorer* (*GALEX*), a NASA Explorer Mission launched on 2003 April 28. *GALEX* is performing the first space UV sky survey, including imaging and grism surveys in two bands (1350–1750 and 1750–2750 Å). The surveys include an all-sky imaging survey ($m_{AB} \simeq 20.5$), a medium imaging survey of 1000 deg^2 ($m_{AB} \simeq 23$), a deep imaging survey of 100 deg^2 ($m_{AB} \simeq 25$), and a nearby galaxy survey. Spectroscopic (slitless) grism surveys ($R = 100$–200) are underway with various depths and sky coverage. Many targets overlap existing or planned surveys in other bands. We will use the measured UV properties of local galaxies, along with corollary observations, to calibrate the relationship of the UV and global star formation rate in local galaxies. We will apply this calibration to distant galaxies discovered in the deep imaging and spectroscopic surveys to map the history of star formation in the universe over the redshift range $0 < z < 2$ and probe the physical drivers of star formation in galaxies. The *GALEX* mission includes a guest investigator program, supporting the wide variety of programs made possible by the first UV sky survey.

Subject headings: galaxies: evolution — galaxies: general — space vehicles: instruments — surveys — ultraviolet: galaxies — ultraviolet: general

1. MOTIVATION FOR *GALEX*

The *Galaxy Evolution Explorer* (*GALEX*), a NASA Small Explorer mission, is performing the first all-sky imaging and spectroscopic surveys in the space ultraviolet (1350–2750 Å).[11] The prime goal of *GALEX* is to study star formation in galaxies and its evolution with time. *GALEX* primary mission surveys, and dedicated observations for the guest investigator program that began in 2004 October, will also support a broad array of other investigations.

1.1. *Galaxy Evolution*

B.-M. Tinsley, in her seminal 1968 paper (Tinsley 1968), demonstrated that passive stellar evolution and an evolving stellar birthrate required to match the properties of nearby galaxies had a profound impact on the appearance of galaxies observed over cosmological distances. It is now doctrine that galaxies cannot be used as standard candles for cosmological tests. The study of distant galaxies has become an exploration of the physical processes that assembled luminous matter in the cores of growing dark matter halos.

Tinsley (1968) observed that the diversity of galaxies we see today is, at its core, a diversity in star formation histories. A central goal of cosmology is to measure and explain the star formation, gas depletion, and chemical evolution history in galaxies. Two major developments in the mid-1990s led new urgency to this goal. The first was the discovery of a population of star-forming Lyman break galaxies (LBGs) at $z \sim 3$ (Steidel et al. 1996). The second was the prediction (Fall et al. 1996), based on QSO absorption-line evolution, and first evidence (Lilly et al. 1996) for strong evolution in the total cosmic star formation rate (SFR). These culminated in the now famous plot (Madau et al. 1996) of cosmic star formation history, which hinted that the SFR density in the universe was 10 times more vigorous and peaked 5–8 Gyr ago. A major goal is to delineate the cosmic star formation history using any and all metrics. As a result of, in part, the diversity of techniques, the current Madau plot remains a weak constraint on cosmogenic models. A parallel effort is now underway to measure the cosmic stellar mass history (Dickinson et al. 2003)—if the stellar initial mass function is universal and constant, these histories must agree.

The rest UV provides a powerful tool for measuring and understanding star formation in galaxies at all epochs, a fact underscored by the discovery and study of LBGs. As emphasized by Adelberger & Steidel (2000), even when dust extinction is great, rest-UV luminosities remain large enough to be detected in UV-selected surveys. The *James Webb Space Telescope* (*JWST*) will extend rest-UV selection to redshifts of 5–20, perhaps the first generation of stars. Ironically, the interpretation of high-redshift galaxies in the rest UV is most limited

[1] California Institute of Technology, MS 405-47, 1200 East California Boulevard, Pasadena, CA 91125.
[2] Jet Propulsion Laboratory, California Institute of Technology, 4800 Oak Grove Drive, Pasadena, CA 91109.
[3] Laboratoire d'Astrophysique de Marseille, BP 8, Traverse du Siphon, 13376 Marseille Cedex 12, France.
[4] Space Sciences Laboratory, University of California at Berkeley, 7 Gauss Way, Berkeley, CA 94720.
[5] Department of Physics and Astronomy, Johns Hopkins University, Homewood Campus, Baltimore, MD 21218.
[6] Center for Space Astrophysics, Yonsei University, Seoul 120-749, Korea.
[7] Observatories of the Carnegie Institution of Washington, 813 Santa Barbara Street, Pasadena, CA 91101.
[8] NASA/IPAC Extragalactic Database, California Institute of Technology, Mail Code 100-22, 770 South Wilson Avenue, Pasadena, CA 91125.
[9] Laboratory for Astronomy and Solar Physics, NASA Goddard Space Flight Center, Greenbelt, MD 20771.
[10] Department of Physics and Astronomy, University of California, Los Angeles, CA 90095.
[11] Note that other missions are performing or plan to perform nebular spectroscopic UV surveys of the diffuse UV sky, for which *GALEX* is obtaining broadband images with 5″ resolution.

by the lack of large, systematic surveys of low-redshift UV galaxies serving as a benchmark.

While the initial conditions that led to structure formation in the universe are becoming clear (de Bernardis et al. 2000; Bennett et al. 2003), the formation and evolution of galaxies are tied to the complex behavior of gas dissipating and cooling within dark matter halos and feedback from massive stars. Fundamentally lacking in numerical simulations and semianalytic models is a predictive physical model for star formation.

1.2. *The UV Sky: Precursors to GALEX*

Technological obstacles have slowed progress in mapping the UV sky to a series of important but incremental advances. The *Orbiting Astronomical Observatory 2* (Code et al. 1970) provided the first systematic UV photometry and spectrophotometry of bright stars, globular clusters, and nearby galaxies. The *TD-1* satellite performed an all-sky spectrophotometric survey of objects to a visual magnitude of 9–10 (Boksenberg et al. 1973). The *Astronomical Netherlands Satellite* (van Duinen et al. 1975) made UV observations of stars, globular clusters, planetary nebulae, and galaxies. The highly successful *International Ultraviolet Explorer* (Kondo 1987), the first satellite mission to use an imaging UV detector, obtained thousands of targeted low- and high-resolution spectra in the 1200–3000 Å band. Along with many other results, these targeted missions provided the foundation for galaxy stellar population synthesis models in the UV.

UV survey experiments, beginning in the 1970s, used intensified film photography and relatively small telescope apertures. Wide-field UV surveys were performed aboard *Skylab* (Henize et al. 1975), by a lunar camera erected by *Apollo 16* astronauts (Carruthers 1973), and by the *Spacelab* FAUST instrument (Bowyer et al. 1993). The Ultraviolet Imaging Telescope (Stecher et al. 1997) obtained a wealth of UV images and results over two Shuttle Astro missions. The balloon-borne FOCA Telescope (Milliard et al. 1992) obtained the first far-UV (FUV) luminosity function for galaxies in the local universe (Treyer et al. 1998) and the first rest-UV anchor point for the star formation history plot.

1.3. *GALEX Goals*

The *GALEX* mission was therefore designed with three overarching primary science goals. All three goals require the primary *GALEX* UV surveys and multiwavelength corollary data. *GALEX* surveys are therefore designed to exploit existing and planned surveys in other bands.

The first goal is to provide a calibration of UV and galaxy SFR, accounting for, in order of declining impact, extinction, starburst history, initial mass function, and metallicity. This calibration would be obtained over a wide range of star formation environments and modalities, so that the relationships can be applied to galaxies at cosmic epochs where star formation may assume a very different character. As we show in Figure 1, the UV provides a measure of star formation on timescales $\sim 10^8$ yr. In galaxies with smoothly varying star formation histories, the UV provides a linear measure of the current SFR once the extinction problem is solved. A major *GALEX* objective is to determine the minimum set of observations required to measure intrinsic extinction, in the spirit of the starburst UV slope–infrared excess relationship of Meurer et al. (1999). In galaxies with more complex star formation histories, the UV probes timescales relevant to starbursts triggered by major interactions and mergers, a core element of hierarchical structure models.

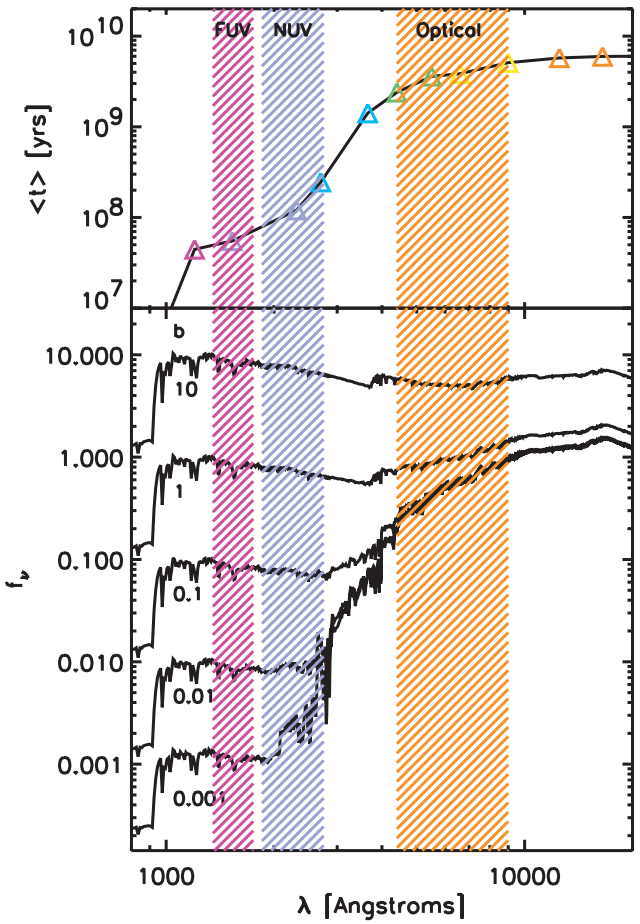

FIG. 1.—*Top*: Flux-weighted age of a simple stellar population from Bruzual & Charlot (2003) vs. wavelength. The UV traces star formation over timescales of $10^{7.5}$–$10^{8.5}$ yr. *Bottom*: Flux from old plus young stellar populations, for values of $b = M/\langle M \rangle$ (the ratio of present to average SFR) ranging from $b = 10$ to $b = 0.001$.

The second *GALEX* goal is to use the rest-UV surveys to determine the cosmic star formation history over the redshift range $0 < z < 2$ (the last 9 Gyr) and its dependence on environment, mass, morphology, merging, and star formation modality (notably quiescent vs. interacting/merging). This history could then be laid side by side with ground, *Hubble Space Telescope*, *JWST*, and other optical–near-IR surveys of rest-UV galaxies at redshifts $1.5 < z < 20$ (the first 4 Gyr) to yield a consistent measurement of galaxy building over the age of the universe. A key strength of rest-UV observations is the decoupling of recent and old star formation histories. As we show in Figure 1, the rest UV scales with SFR over a very wide range of specific SFRs, parameterized by b, the ratio of present to average SFRs over the life of the galaxy.

Finally, the third *GALEX* goal is to use both large statistical samples and detailed studies of nearby galaxies, again with abundant multiwavelength data, to inform and inspire a predictive model of global SFRs in diverse contexts.

2. MISSION OVERVIEW

2.1. *Observatory Design*

The *GALEX* instrument employs a novel optical design using a 50 cm diameter modified Ritchey-Chrétien telescope with four

TABLE 1

GALEX On-Orbit Performance

Parameter	Value
Effective area	20–50 cm^2
Angular resolution	4.″5–6″ FWHM
Spectral resolution	100–250
Field of view	1.°2
Bands (simultaneous)	FUV 1350–1750 Å; NUV 1750–2750 Å
Sensitivity (AB mag)	100 s 20.5 (AIS)
	1 ks 23.5 (MIS/NGS)
	30 ks 25.5 (DIS)
Astrometry	1″ (rms)
Observations	Nighttime—1 eclipse = 1000–2000 s
Mission length	Baseline 38 months, 13 months to date

channels: FUV and near-UV (NUV) imaging and FUV and NUV spectroscopy. The telescope has a 3 m focal length and is coated with Al-MgF_2. The field of view is 1.°2 circular. An optics wheel places a CaF_2 imaging window, a CaF_2 transmission grism, or an opaque position in the beam. Spectroscopic observations are obtained at multiple grism-sky dispersion angles, also selectable, to remove spectrum overlap effects. The FUV (1350–1750 Å) and NUV (1750–2750 Å) bands are obtained simultaneously using a dichroic beam splitter that also acts as a field aberration corrector. The beam splitter/asphere is an ion-etched fused-silica plate with aspheric surfaces on both sides. Beam splitting is accomplished with a dielectric multilayer on the input side, which reflects the FUV band and transmits the NUV band. The detector system (provided by a team led by the University of California at Berkeley including Caltech, JPL, and Southwest Research) incorporates sealed tube microchannel plate detectors with a 65 mm active area and crossed delay-line anodes for photon event position readout. The FUV detector is preceded by a blue-edge filter that blocks the nightside airglow lines of O I λλ1304, 1356, and Lyα. The NUV detector is preceded by a red blocking filter/fold mirror, which produces a sharper long-wavelength cutoff than the detector CsTe photocathode and thereby reduces the zodiacal light background and optical contamination. The NUV detector has an MgF_2 window that includes power for field flattening and an opaque CsI photocathode on the microchannel plate. The NUV detector has a fused silica window that also includes power for field flattening and a semitransparent Cs_2Te photocathode on the window inner surface proximity focused across a 300 μm gap. The detector peak quantum efficiency is 12% (FUV) and 8% (NUV). In-orbit, dark background is low, 20/60 counts s^{-1} (FUV/NUV) for diffuse background, as compared to the lowest total night-sky backgrounds of 1500/10,000 counts s^{-1}. The detectors are linear up to a local (stellar) count rate of 100 counts s^{-1} (FUV) and 400 counts s^{-1} (NUV), which corresponds to $m_{AB} \sim 14$–15. The system angular resolution, which includes contributions from the optical and detector point-spread function (PSF), and ex post facto aspect reconstruction, is typically 4.″5/6.″0 (FUV/NUV) (FWHM) and varies by ~20% over the field of view owing to variations in the detector resolution. The grism, fabricated by Jobin-Yvon in Paris, is a ruled CaF_2 prism with a small curvature on the input side. In order to provide simultaneous coverage of the 1350–2750 Å range, the grism is blazed in first order for the NUV band and in second order for the FUV band and obtains peak absolute efficiencies of 80% and 60%, respectively. Spectral resolution is 200/100 (FUV second order/NUV first order). On-orbit angular resolution and instrument throughput are as expected from ground calibration. A more complete description of the instrument and satellite can be found in Martin et al. (2003).

TABLE 2

Survey Summary

Survey	Area (deg^2)	Exposure (ks)	m_{AB}	Number of Galaxies (Estimate)	Volume (Gpc^3)	$\langle z \rangle$
AIS	40000	0.1	20.5	10^7	1	0.1
MIS	1000	1.5	23	$10^{6.5}$	1	0.6
DIS	80	30	25	107	1.0	0.85
UDIS	1	200	26	$10^{5.5}$	0.05	0.9
NGS	...	0.5	27.5[a]	200	...	...
WSS	80	30	20	10^4–10^5	0.03	0.15
MSS	8	300	21.5[b]	10^4	0.03	0.3
	8	300	23.3[c]	10^5	0.03	0.5
DSS	2	2000	22.5[b]	10^4	0.05	0.5
	2	2000	24.3[c]	10^5	...	0.9

[a] Magnitude in units of $arcsec^2$.
[b] $R = 100$.
[c] $R = 20$.

2.2. *Mission Operations*

GALEX was launched by a Pegasus-XL vehicle on 2003 April 28 into a 29° inclination, 690 km circular, 98.6 minute period orbit. *GALEX* began nominal operations on August 2. A summary of on-orbit performance is given in Table 1, and more details on the on-orbit performance are given in the following Letter by Morrissey et al. (2005). The eight surveys listed in Table 2 are being performed concurrently for the first 38 months. The mission design is simple. Science data is obtained only on the nightside. On the dayside, the satellite is in solar panel–Sun orientation. As the satellite enters twilight, it slews to one of the survey targets. The imaging window or grism is selected, and the detector high voltage is ramped from idle. All observations are performed in a pointed mode with an arcminute spiral dither to average nonuniformities and to prevent detector fatigue by bright stars. Individual photon events, time-tagged to 1–5 ms accuracy, are stored on the spacecraft solid-state tape recorder along with housekeeping data. At the end of each orbital night, detector high voltages are ramped back to idle levels to protect detectors from damage and the spacecraft returns to solar array pointed attitude. Up to four times per 24 hr day, the solid-state recorder is dumped via the X-band transmitter to ground stations in Hawaii or Perth, Australia.

The *GALEX* data analysis pipeline operated at the Caltech Science Operations Center receives the time-tagged photon lists, instrument/spacecraft housekeeping, and satellite aspect information. From these data sets, the pipeline reconstructs the aspect versus time and generates images, spectra, and source catalogs. The first pipeline module corrects the photon positions for detector and optical distortions and calculates an optimal aspect solution based on the time-tagged photon data and star catalogs. A photometric module accumulates the photons into count, intensity, and effective area maps and extracts sources using the well-known SExtractor program, augmented by significant preprocessing of the input images as well as postprocessing the resulting source catalog. A spectroscopic module uses *GALEX* image source catalog inputs to extract spectra of these sources from the multiple slitless grism observations.

2.3. *Survey Design*

Night-sky backgrounds in the *GALEX* bands are low: the FUV (NUV) is dominated by diffuse galactic light (zodiacal light), with typical levels 27.5 (26.5) mag $arcsec^{-2}$, corresponding to 3 (30) photons per PSF in one eclipse. Surveys become background limited at $m_{AB} \sim 23.5$. Targets are constrained by the current bright star limit for the detectors (5 kilocounts s^{-1}),

which makes 50% of the sky inaccessible. With the NUV detector off, 72% of the sky is accessible. This limit will be raised to 50 kilocounts s^{-1} shortly after ground verification tests. With this new limit, 95% of the sky can be surveyed in FUV-only mode, and 87% with both detectors operating.

All-sky Imaging Survey (AIS).—The goal of the AIS is to survey the entire sky subject to a sensitivity of $m_{AB} \simeq 20.5$, comparable to the Palomar Observatory Sky Survey II ($m_{AB} = 21$) and Sloan Digital Sky Survey (SDSS) spectroscopic ($m_{AB} = 17.6$) limits. Several hundred to 1000 objects are in each 1 deg^2 field. The AIS is performed in roughly 10 100 s pointed exposures per eclipse ($\sim$10 deg^2 per eclipse).

Medium Imaging Survey (MIS).—The MIS covers 1000 deg^2, with extensive overlap of the SDSS. MIS exposures are a single eclipse, typically 1500 s, with sensitivity $m_{AB} \simeq 23$, net several thousand objects, and are well matched to SDSS photometric limits.

Deep Imaging Survey (DIS).—The DIS consists of 20 orbit (30 ks, $m_{AB} \simeq 25$) exposures, over 80 deg^2, located in regions where major multiwavelength efforts are already underway. DIS regions have low extinction, low zodaical, and diffuse galactic backgrounds, contiguous pointings of 10 deg^2 to obtain large cosmic volumes, and minimal bright stars. An Ultra-Deep Imaging Survey (UDIS) of 200 ks, $m_{AB} \sim 26$, is also in progress in four fields.

Nearby Galaxies Survey (NGS).—The NGS targets well-resolved nearby galaxies for 1–2 eclipses. Surface brightness limits are $m_{AB} \sim 27.5$ $arcsec^{-2}$, or an SFR of 10^{-3} $M_\odot$ yr^{-1} kpc^{-2}. The 200 targets are a diverse selection of galaxy types and environments and include most galaxies from the *Spitzer* IR Nearby Galaxy Survey (SINGS). Figure 2 shows the NGS observation of the M81/M82 system.

Spectroscopic surveys.—The suite of spectroscopic surveys includes (1) the Wide-field Spectroscopic Survey (WSS), which covers the full 80 deg^2 DIS footprint with comparable exposure time (30 ks) and reaches $m_{AB} \sim 20$ for spectra with signal-to-noise ratios of $\sim$10 spectra; (2) the Medium-deep Spectroscopic Survey (MSS), which covers the high-priority central field in each DIS survey region (total 8 deg^2) to $m_{AB} = 21.5$–23, using 300 ks exposures; and (3) the Deep Spectroscopic Survey (DSS), covering 2 deg^2 with 1000 eclipses, to a depth of $m_{AB} = 23$–24.

3. EARLY RESULTS

In this dedicated *Astrophysical Journal Letters* issue, we describe a selection of early results obtained from the *GALEX* surveys. In this introductory Letter, we give examples of data from the various surveys and highlight some of the early results described in more detail in this issue.

3.1. *Star Formation in Diverse Contexts*

GALEX observations demonstrate that rest-UV emission traces star formation in a wide variety of contexts, environments, and modalities. In nearby quiescent disk galaxies (M101, M51, M33), *GALEX* observations provide the ages, luminosities, masses, and extinction of star formation complexes. These show that the cluster age distribution is consistent with a constant SFR over the last 10^9 Myr (Bianchi et al. 2005a; Thilker et al. 2005a).

GALEX has discovered extended UV emission far outside (2–4 times) the optical disk of a number of nearby spiral galaxies, including M83 and NGC 628. Star formation appears to proceed at gas surface densities below the typical galaxian threshold, and the complexes formed appear to have lower luminosity and mass and younger ages than those in the inner disk (Thilker et al. 2005b).

In the Antennae merger system, recent star formation has occurred in the disk, tails, and Tidal Dwarf galaxy on timescales less than the 300 Myr dynamical time, implying that star formation is triggered in the tidal streams after gas leaves the galaxy (Hibbard et al. 2005). *GALEX* has detected UV emission in extended tidal tails of a number of other interacting galaxies (Neff et al. 2005a; Xu et al. 2005b) showing ages less than interaction times, suggesting that interaction-induced star formation in tidal gas streams may be a common phenomenon. All of these phenomena are likely to be more common at high redshift.

3.2. *Star Formation History*

Large-area, unbiased, multiwavelength surveys support a robust statistical study of the fundamental properties of galaxies. *GALEX* provides an unprecedented measurement of SFRs. When combined with rest-optical/near-IR, the key parameter of the SFR per unit stellar mass (specific SFR), which is closely related to the current SFR with respect to the average (the *b*-parameter), can be determined over a wide dynamic range.

GALEX combined with the SDSS forms a powerful data set. *GALEX*-SDSS colors provide preliminary source classification and characterization (Seibert et al. 2005a; Bianchi et al. 2005b), separating main-sequence, post–main-sequence, and binary stars, QSOs, and galaxies. *GALEX*/SDSS photometry provides excellent measurements of the ratio of current to average SFRs (the *b*-parameter) and important constraints on starburst history in the local universe (Salim et al. 2005).

In the local universe, UV luminosities follow a Schechter function with $L_* = 2 \times 10^9$ $L_\odot$ (Wyder et al. 2005), with measureably different parameters for red and blue subsamples and evidence for evolution (Treyer et al. 2005). The luminosity functions and densities are significantly fainter than those obtained by FOCA. *GALEX* on-orbit calibration shows excellent agreement with the ground calibration (Morrissey et al. 2005), so we attribute this discrepancy to an overestimate of fluxes at faint magnitudes by FOCA. *GALEX* number count distributions fall below those of FOCA, show some evidence for evolution, and show some flattening at faint magnitudes due to a combination of blending, confusion, and faint wing overlap (Xu et al. 2005a).

GALEX DIS data, combined with the Very Large Telescope Visible Multiobject Spectrograph redshift survey, has provided the first *GALEX* measurements of the evolution of the UV luminosity function and density (Arnouts et al. 2005). Significant evolution is found, consistent with $\sim(1 + z)^2$. When corrected for extinction using the Kong et al. (2004) prescription, this provides the first *GALEX* measurements of cosmic SFR history over $0 < z < 1.2$ (Schiminovich et al. 2005). When combined with consistent analysis of deep optical data from the Hubble Deep Field–North (Arnouts et al. 2005; Schiminovich et al. 2005), the results suggest a monotonic decline in the SFR density since $z = 3$, rather than a peak at $z \sim 1$–1.5.

The *GALEX* AIS/MIS-SDSS data release 1 matched data sets have yielded the discovery of luminous UV galaxies (LUGs), with UV luminosities and properties comparable to distant LBGs, in the local universe (Heckman et al. 2005). LUGs have 500 times lower volume density than LBGs, but their density rises sharply toward higher redshift (Schiminovich et al. 2005). LUGs may provide an excellent opportunity to study low-redshift analogs to massive star-forming galaxies at high redshift.

3.3. *Dust Extinction*

UV extinction by dust remains the principle obstacle in converting UV luminosity directly to the SFR. In individual galaxies (M83 and M101), we show that extinction is a strongly declining function of radius and may contain a significant diffuse, interarm component (Popescu et al. 2005; Boissier et al. 2005).

With *IRAS* data, we have begun to characterize the properties of FUV and far-IR–selected galaxy samples in the local universe. As expected, flux-limited UV and far-IR–selected samples yield different projections of the bivariate UV/far-IR luminosity function and distinct UV/far-IR ratios (Buat et al. 2005). However, virtually all star-forming galaxies detected in local far-IR–selected samples are also detected by *GALEX*. The SFR luminosity function places a fundamental constraint on cosmological models. The bivariate UV/far-IR luminosity function, obtained from combined UV and far-IR–selected samples, shows a bimodal behavior: $L_{\rm FUV}$ tracks $L_{\rm FIR}$ for $L_{\rm tot} < 3 \times 10^9\ L_{\odot}$, and $L_{\rm FUV}$ saturates for higher total luminosities. The total SFR function is a lognormal function over four decades of luminosity (Martin et al. 2005).

Starburst galaxies in the local universe display a well-known relationship between UV slope (β) and far-IR–to–UV luminosity ratio (IRX). Early results from *GALEX* (Seibert et al. 2005b) indicate that normal and quiescent star-forming galaxies fall below the canonical IRX-β relation for starbursts but that the deviation does not correlate strongly with starburst age (Kong et al. 2004) or other observables.

3.4. *UV from Stars, Gas, Dust, and AGNs*

In addition to recent star formation, the UV traces dust through scattering and absorption, gas by emission lines and two-photon continuum, hot evolved stars (Rey et al. 2005) and late-type stellar chromospheres, degenerate binaries, and QSOs. Early-type galaxies, such as M32, show modest color gradients (Gil de Paz et al. 2005) that probably trace metallicity. While some 15%–20% of "normal" elliptical galaxies show evidence for residual star formation at the 1%–2% level (Yi et al. 2005), quiescent elliptical galaxies (notably in rich clusters) exhibit the well-known UV excess but without the previously claimed correlation with metallicity (Rich et al. 2005). Distant elliptical galaxies show evidence for evolution in the UV-rising flux (Lee et al. 2005). The M82 outflow, prominent in Figure 2, is injecting abundant dust into the intergalactic medium, which reflects the UV from the obscured starburst (Hoopes et al. 2005). As the AIS progresses, the number of QSOs suitable for measurements of He II reionization are increasing.

4. *GALEX* DATA LEGACY

GALEX early release data was made available in 2003 December. The first major data release, GDR1, occurred on 2004 October 1, coincident with the start of the *GALEX* guest investigator program. All *GALEX* data are served by the Multimission Archive at the Space Telescope Science Institute. While we cannot predict the applications to which the *GALEX* data will be applied in the future, we can anticipate that the impacts of the first comprehensive UV sky survey will be broad and lasting.

GALEX is a NASA Small Explorer, launched in 2003 April. We gratefully acknowledge NASA's support for construction, operation, and science analysis for the *GALEX* mission, developed in cooperation with the Centre National d'Etudes Spatiales of France and the Korean Ministry of Science and Technology. The grism, imaging window, and uncoated aspheric corrector were supplied by France. We acknowledge the dedicated team of engineers, technicians, and administrative staff from JPL/Caltech, Orbital Sciences Corporation, University of California, Berkeley, Laboratory Astrophysique Marseille, and the other institutions who made this mission possible.

REFERENCES

Adelberger, K. L., & Steidel, C. C. 2000, ApJ, 544, 218
Arnouts, S., et al. 2005, ApJ, 619, L43
Bennett, C. L., et al. 2003, ApJ, 583, 1
Bianchi, L., et al. 2005a, ApJ, 619, L71
———. 2005b, ApJ, 619, L27
Boissier, S., et al. 2005, ApJ, 619, L83
Boksenberg, A., et al. 1973, MNRAS, 163, 291
Bowyer, S., Sasseen, T. P., Lampton, M., & Wu, X. 1993, ApJ, 415, 875
Bruzual, G., & Charlot, S. 2003, MNRAS, 344, 1000
Buat, V., et al. 2005, ApJ, 619, L51
Carruthers, G. R. 1973, Appl. Opt., 12, 2501
Code, A. D., Houck, T. E., McNall, J. F., Bless, R. C., & Lillie, C. F. 1970, ApJ, 161, 377
de Bernardis, P., et al. 2000, Nature, 404, 955
Dickinson, M., Papovich, C., Ferguson, H. C., & Budavári, T. 2003, ApJ, 587, 25
Fall, S. M., Charlot, S., & Pei, Y. C. 1996, ApJ, 464, L43
Gil de Paz, A., et al. 2005, ApJ, 619, L115
Heckman, T., et al. 2005, ApJ, 619, L35
Henize, K. G., Wray, J. D., Parsons, S. B., Benedict, G. F., Bruhweiler, F. C., Rybski, P. M., & Ocallaghan, F. G. 1975, ApJ, 199, L119
Hibbard, J., et al. 2005, ApJ, 619, L87
Hoopes, C., et al. 2005, ApJ, 619, L99
Kondo, Y., ed. 1987, Exploring the Universe with the *IUE* Satellite (Dordrecht: Reidel)
Kong, X., Charlot, S., Brinchmann, J., & Fall, S. M. 2004, MNRAS, 349, 769
Lee, Y.-W., et al. 2005, ApJ, 619, L103
Lilly, S. J., Le Fèvre, O., Hammer, F., & Crampton, D. 1996, ApJ, 460, L1
Madau, P., Ferguson, H. C., Dickinson, M. E., Giavalisco, M., Steidel, C. C., & Fruchter, A. 1996, MNRAS, 283, 1388
Martin, C., et al. 2003, Proc. SPIE, 4854, 336
Martin, D. C., et al. 2005, ApJ, 619, L59
Meurer, G. R., Heckman, T. M., & Calzetti, D. 1999, ApJ, 521, 64
Milliard, B., Laget, M., & Donas, J. 1992, IAU Commission Instrum., 2, 49
Morrissey, P., et al. 2005, ApJ, 619, L7
Neff, S., et al. 2005, ApJ, 619, L91
Popescu, C., et al. 2005, ApJ, 619, L75
Rey, S.-C., et al. 2005, ApJ, 619, L119
Rich, R. M., et al. 2005, ApJ, 619, L107
Salim, S., et al. 2005, ApJ, 619, L39
Schiminovich, D., et al. 2005, ApJ, 619, L47
Seibert, M., et al. 2005a, ApJ, 619, L23
———. 2005b, 619, L55
Stecher, T. P., et al. 1997, PASP, 109, 584
Steidel, C. C., Giavalisco, M., Pettini, M., Dickinson, M., & Adelberger, K. L. 1996, ApJ, 462, L17
Thilker, D., et al. 2005a, ApJ, 619, L67
———. 2005b, ApJ, 619, L79
Tinsley, B. M. 1968, ApJ, 151, 547
Treyer, M. A., Ellis, R. S., Milliard, B., Donas, J., & Bridges, T. J. 1998, MNRAS, 300, 303
Treyer, M., et al. 2005, ApJ, 619, L19
van Duinen, R. J., Aalders, J. W. G., Wesselius, P. R., Wildeman, K. J., Wu, C. C., Luinge, W., & Snel, D. 1975, A&A, 39, 159
Wyder, T., et al. 2005, ApJ, 619, L15
Xu, C. K., et al. 2005a, ApJ, 619, L95
———. 2005b, ApJ, 619, L11
Yi, S. Y., et al. 2005, ApJ, 619, L111

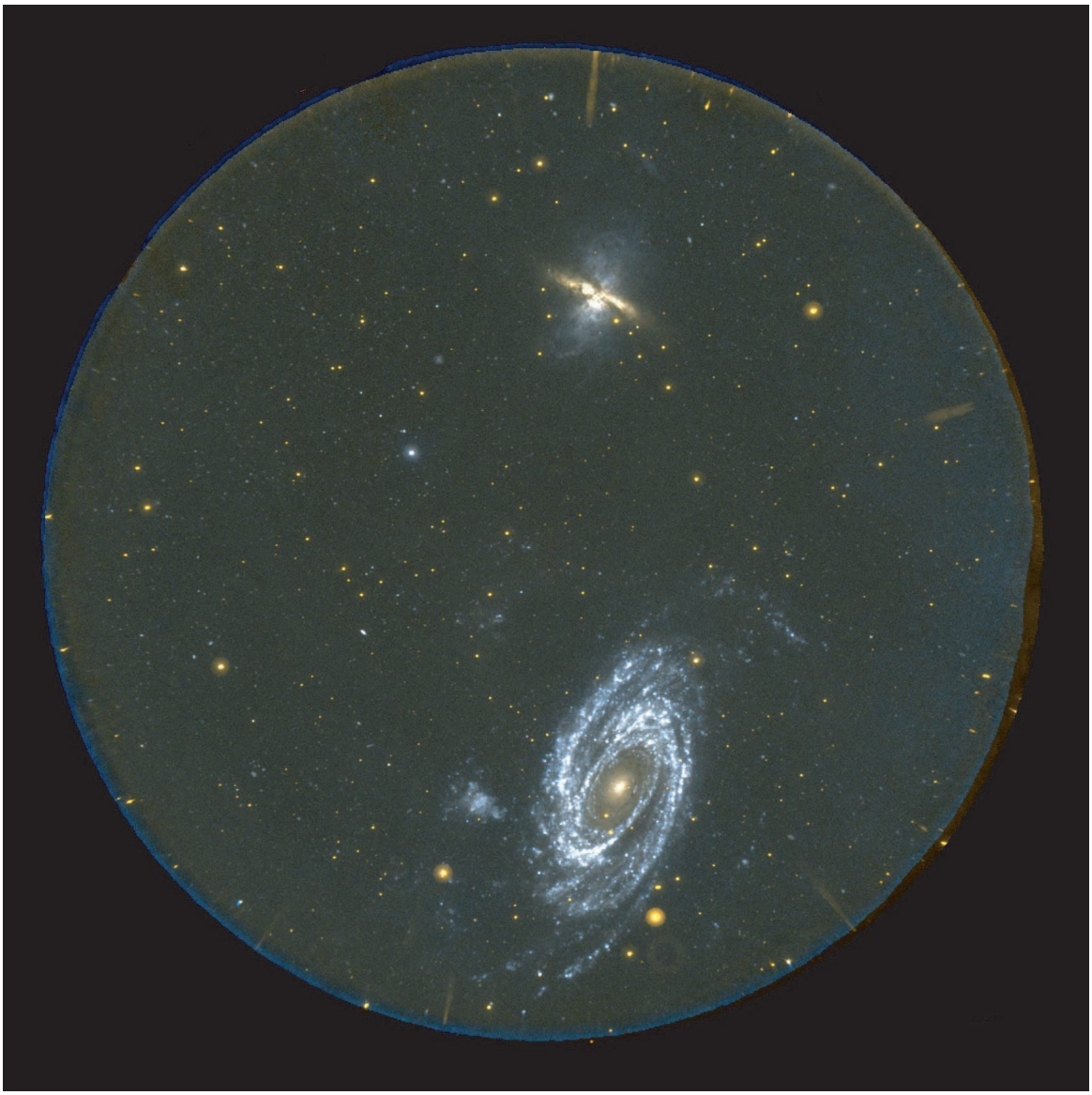

FIG. 2.—*GALEX* NGS observation of the M81-M82 system. This figure illustrates how a single *GALEX* image may be used to study many different aspects of galaxy evolution: spiral structure, stellar populations, extinction (M81), interaction-induced starbursts, and resulting galactic outflows (M82); star formation in dwarf galaxies (Ho IX), between galaxies and in tidal streams; the UV background; and large-scale structure. In the color table, red-green (gold) is used for NUV, and blue for FUV.